

Photoluminescence studies of Si-doped AlN epilayers

K. B. Nam, M. L. Nakarmi, J. Li, J. Y. Lin, and H. X. Jiang^{a)}

Department of Physics, Kansas State University, Manhattan, Kansas 66506-2601

(Received 28 May 2003; accepted 10 August 2003)

Si-doped AlN epilayers were grown by metalorganic chemical vapor deposition on sapphire substrates. Deep ultraviolet picosecond time-resolved photoluminescence (PL) spectroscopy has been employed to study the optical transitions in the grown epilayers. The donor bound exciton (I_2) transition was found to be the dominant recombination line in Si-doped AlN epilayers at 10 K and its emission intensity decreases with increasing Si dopant concentration. Doping-induced PL emission linewidth broadening and band-gap renormalization effects have also been observed. Time-resolved PL studies revealed a linear decrease of PL decay lifetime with increasing Si dopant concentration, which was believed to be a direct consequence of the doping-enhanced nonradiative recombination rates. © 2003 American Institute of Physics. [DOI: 10.1063/1.1616199]

With the tremendous progress of III-nitride research and development in terms of both fundamental understanding as well as device applications, AlN emerges as an important wide band-gap semiconductor material. AlN and Al-rich Al-GaN alloys, covering wavelengths down to 200 nm, are ideal materials for the development of chip-scale ultraviolet (UV) light sources/sensors, because AlGaN is the only wide band-gap semiconductor system that possesses the ability of band-gap engineering through the use of alloying and heterostructure design. AlN has many other attractive properties,^{1,2} such as high mechanical hardness and thermal conductivity, large dielectric constant, and high resistance to harsh conditions. In spite of the recognition of the importance of AlN, many of its fundamental optical properties, particularly the recombination dynamics associated with free carriers, excitons, and band-to-impurity transitions in AlN, are still largely unknown due to the lack of high quality materials as well as technical difficulties involved in the deep UV (down to 200 nm) time-resolved photoluminescence (PL) measurements.

Recently, our group has obtained undoped AlN epilayers with high optical qualities on sapphire substrates by metalorganic chemical vapor deposition (MOCVD). Very efficient band-edge PL emission lines have been observed with above band-gap excitation.³ We have developed a deep UV picosecond time-resolved optical spectroscopy system for probing the emission properties of III-nitrides with high Al contents with a time-resolution of a few ps and wavelength down to deep UV (195 nm) to cover pure AlN. A value of about 80 meV for the free exciton binding energy in AlN was deduced from time-resolved PL studies, with a large free exciton binding energy in semiconductors, implying that excitons in AlN are an extremely robust system that would survive well above room temperature.⁴ This together with other well-known physical properties of AlN may considerably expand future prospects for the application of III-nitride materials.

The availability of AlN epilayers with high optical quality and deep UV picosecond time-resolved PL system opens the possibility for us to probe the recombination dynamics

associated with fundamental optical transitions in AlN. In this letter we present the results of MOCVD growth of Si doped AlN epilayers and the results of deep UV picosecond time-resolved PL studies. Doping-induced PL emission linewidth broadening, enhanced nonradiative decay rate, and band-gap renormalization have been observed.

The 1 μm thick Si-doped AlN epilayers were grown by MOCVD on sapphire (0001) substrates with low temperature AlN nucleation layers. Trimethylaluminum (TMAI), NH_3 , and SiH_4 were used as Al, N, and Si sources. Atomic force microscopy (AFM) was employed to examine the surface morphologies of the grown epilayers. The deep UV laser spectroscopy system used for picosecond time-resolved PL studies consists of a frequency quadrupled 100 fs Ti:sapphire laser with an excitation photon energy set around 6.28 eV (with a 76 MHz repetition rate and a 3 mW average power), a monochromator (1.3 m), and a streak camera with a detection capability ranging from 185 to 800 nm and a time resolution of 2 ps.⁵ Secondary ion mass spectroscopy (SIMS) measurements (performed by Charles Evans & Associates) indicated that the Si dopant concentration, N_{Si} , in the grown layers varied from 1.5×10^{17} to $1.5 \times 10^{18} \text{ cm}^{-3}$. However, Hall effect measurements have shown that all layers were highly resistive.

Figure 1 shows the low-temperature (10 K) PL spectra of Si-doped AlN epilayers with different Si dopant concentrations, N_{Si} . For the lightly doped sample, $N_{\text{Si}} = 1.5 \times 10^{17} \text{ cm}^{-3}$, two emission peaks (with Gaussian shapes) are well resolved and we assign the emission line at 6.024 eV to the donor bound exciton (I_2) transition. The temperature dependence of the PL emission characteristics as well as the PL decay lifetime measurements further confirm this assignment.⁴ The general trends seen for the I_2 transition are that its emission intensity decreases whereas the FWHM increases with increasing N_{Si} . Furthermore, Si doping also induces a redshift in the spectral peak position of the I_2 emission line. These results are more clearly illustrated in Fig. 2, where the integrated PL intensity, FWHM, and the spectral peak position of the I_2 emission line as functions of N_{Si} are depicted.

^{a)}Electronic mail: jjiang@phys.ksu.edu

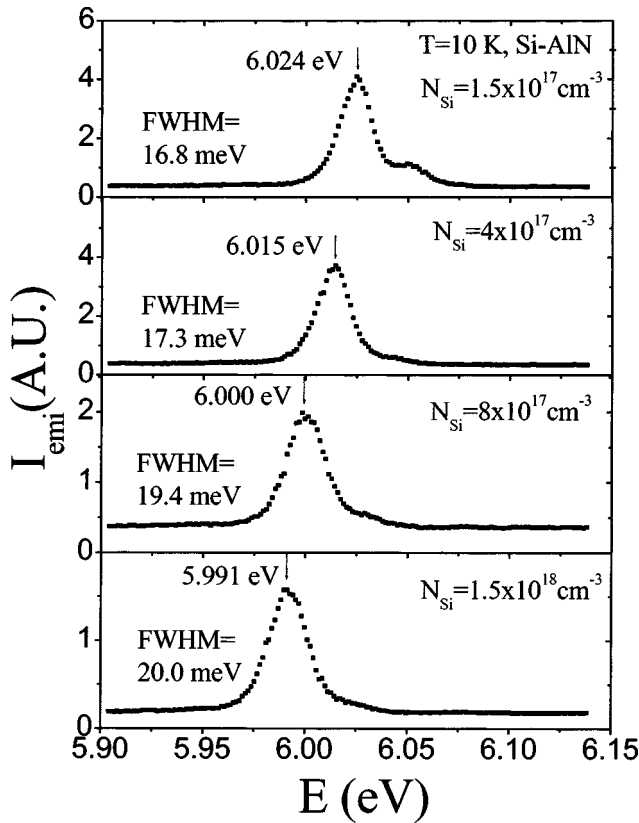


FIG. 1. Low-temperature (10 K) PL spectra of the band-edge transitions in Si-doped AlN with different Si-doping concentrations, N_{Si} .

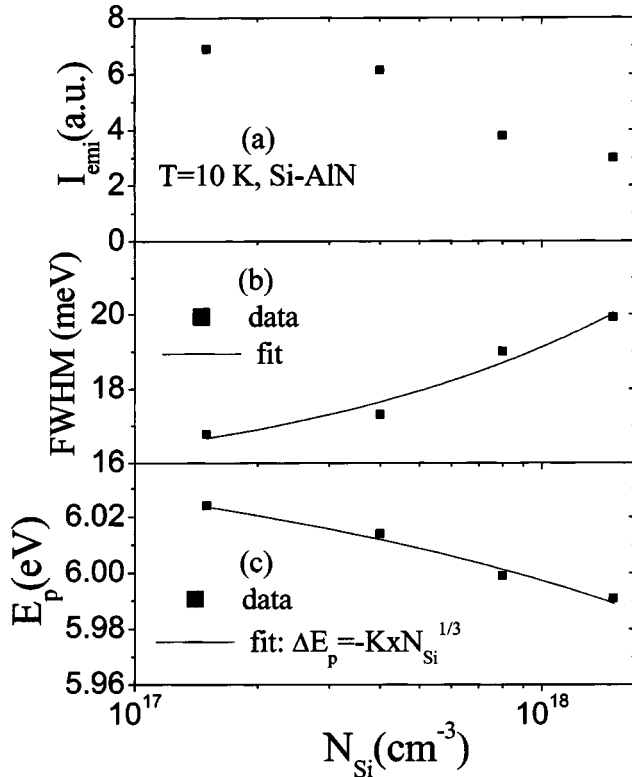


FIG. 2. (a) Integrated PL intensity, (b) full width at half maximum (FWHM), and (c) the PL energy peak position of the I_2 emission line, E_p , as functions of N_{Si} in Si-doped AlN epilayers and the solid line is the least-squares fit of data with Eq. (2).

Figure 2(a) shows that the I_2 emission intensity decreases continuously with increasing N_{Si} . This implies an increased defect density as well as a reduced materials quality with an increase of N_{Si} . This fact contrasts the results obtained for GaN, in which Si doping in general improves the material quality and the PL emission intensity.^{6–8} AFM studies also reveal that the root mean square (rms) of surface morphology increases with increasing N_{Si} , varying from 0.7 nm for $N_{\text{Si}}=0$ –6 nm for $N_{\text{Si}}=1.5 \times 10^{18} \text{ cm}^{-3}$, indicating a reduced material quality with increasing N_{Si} and corroborating the PL results. The I_2 transition line can be described by a model that accounts for the emission line width broadening due to local potential fluctuations induced by random distributions of doping impurities:^{6,7}

$$\text{FWHM} = E_0 + \alpha \sqrt{N_{\text{Si}} r_s}, \quad (1)$$

where E_0 is the FWHM at $N_{\text{Si}}=0$, α a constant depending on materials, and r_s the Debye or Thomas–Fermi screening radius for nondegenerate and degenerate doping concentrations, respectively. The solid line is the least-squares fit of data with Eq. (1). The fitted value of E_0 is 15.1 meV, which is in excellent agreement with the FWHM (15.5 meV) of the I_2 transition in undoped AlN.⁴

Si doping also induces band-gap renormalization. Figure 2(c) shows that the spectral energy peak position (E_p) of the I_2 emission line decreases (i.e., is redshifted) with an increase of N_{Si} in Si-doped AlN epilayers. Band-gap renormalization is usually due to free carrier screening and is written as $\Delta E_p = -Kn^{1/3}$, where ΔE_p is the reduction of the band gap, n is the electron concentration, and K is a proportionality constant depending on materials.^{9–11} However, no free electrons were found in these samples since all of our AlN epilayers studied here exhibit a high resistivity. The band-gap reduction in this case is presumably due to the screening of ionized impurities, implying that Si doped AlN epilayers grown here are highly compensated. In such a context, ΔE_p is assumed to be proportional to N_{Si} for compensated materials:

$$\Delta E_p = -KN_{\text{Si}}^{1/3}. \quad (2)$$

The dotted line in Fig. 2(c) is the least-squares fit of data with Eq. (2) and clearly shows the effect of doping-induced band-gap renormalization in Si-doped AlN epilayers.

The temperature evolution of the PL spectra has been studied. Figure 3 shows that the dominant emission line in Si-doped AlN evolves from the I_2 to the free exciton (FX) transition with increasing temperature. This is expected since the donor bound excitons dissociate into free excitons (FX) and neutral donors, which is consistent with the results seen in Si-doped GaN and also in undoped AlN in which I_2 is the dominant transition at low temperatures.^{4,11} The absolute emission intensity of the FX transition line also decreases with increasing N_{Si} . The spectral peak positions of both the I_2 and FX transitions are redshifted with increasing temperature and can be written as $E_p(\text{FX}) = E_g - E_x + \alpha k_B T$ and $E_p(I_2) = E_g - E_x - E_{bx}$, respectively, where E_x and E_{bx} are the binding energies of the free exciton and donor-bound exciton, respectively, and α is a constant. Therefore, the en-

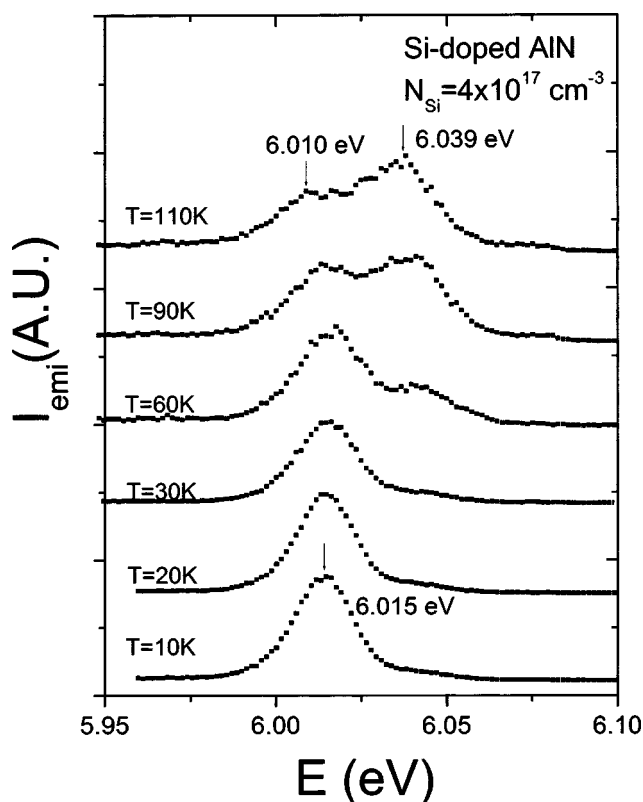


FIG. 3. PL spectra measured at different temperatures for Si-doped AlN epilayer with $N_{\text{Si}} = 4 \times 10^{17} \text{ cm}^{-3}$. The arrows indicate the PL spectral peak positions of the I_2 and FX transitions. The dissociation of the bound excitons with increasing temperature is clearly resolved.

ergy separation between the FX and the I_2 transitions is expected to increase with increasing temperature and can be written as

$$\Delta E_p = E_p(\text{FX}) - E_p(I_2) = E_{bx} + \alpha k_B T. \quad (3)$$

The fitted value of α was obtained to be 0.56.

The PL temporal responses of AlN-epilayers with different Si doping levels have been measured at their respective spectral peak positions and the results are shown in Fig. 4(a). Figure 4(b) shows that the PL decay lifetime, τ , decreases linearly with increasing N_{Si} . In Fig. 4(b), the solid line is a linear fit of the experimental data. The fitted value of $\tau = 82$ ps at $N_{\text{Si}} = 0$ is also in excellent agreement with the decay lifetime (80 ps) of the I_2 transition in undoped AlN.⁴ We believe that the linear decrease of PL decay lifetime with N_{Si} is associated with an increased nonradiative recombination rate with increasing N_{Si} , which corroborates the PL intensity decreasing with N_{Si} shown in Fig. 2(a).

In summary, we have investigated the optical properties of Si-doped AlN epilayers grown on sapphire by MOCVD. The donor-bound exciton (I_2) transition was found to be the dominant transition in these epilayers at 10 K and its emission intensity decreased with increasing Si-doping concentration, N_{Si} . The FWHM of the I_2 transition line measured at 10 K increased with increasing N_{Si} and displayed a $(N_{\text{Si}})^{1/2}$ dependence, due to the local potential fluctuations caused by randomly distributed doping impurities. The doping induced band-gap renormalization effect has also been observed, despite the fact that Si doping did not convert highly insulating

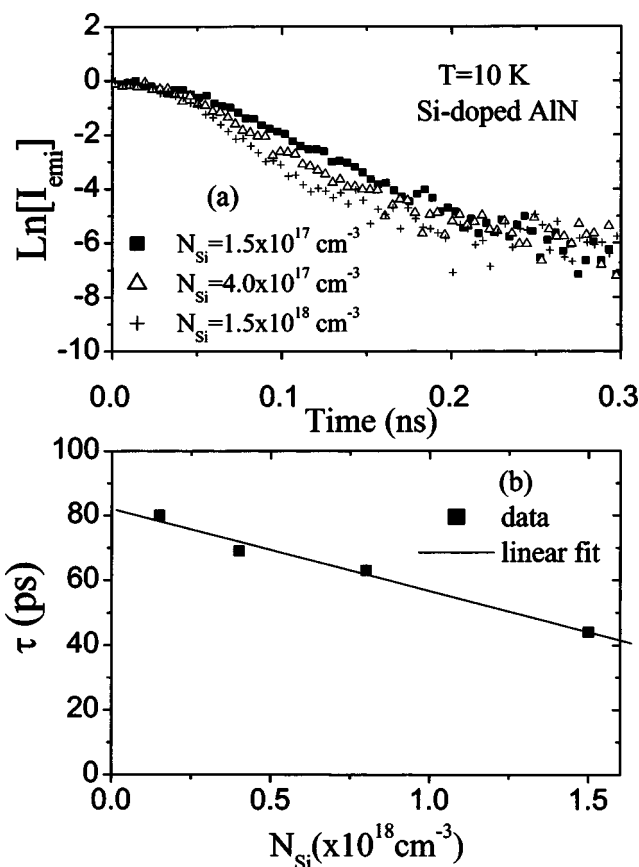


FIG. 4. (a) Temporal responses of the I_2 recombination line in Si-doped AlN epilayers with different N_{Si} measured at their respective spectral peak positions; (b) PL decay lifetime as a function of N_{Si} . The solid line is a linear fit of the experimental data.

AlN to n type. The results thus point to the fact that Si doped AlN epilayers grown here are highly compensated. Time-resolved PL measurements revealed that the recombination lifetime of the I_2 transition decreases linearly with N_{Si} , indicating an increased nonradiative recombination rate at higher doping levels, which is consistent with PL intensity results.

This research is supported by grants from NSF (DMR-0203373), ARO, DOE (DE-FG03-96ER 45604), DARPA, MDA, and ONR.

¹ *Properties of Advanced Semiconductor Materials*, edited by M. E. Levinstein, S. L. Ramyantsev, and M. S. Shur (Wiley, New York, 2001), p. 31.

² *Gallium Nitride and Related Semiconductors*, edited by J. H. Edgar, S. Strite, I. Akasaki, H. Amano, and C. Wetzel (INSPEC, London, 1999).

³ J. Li, K. B. Nam, M. L. Nakarmi, J. Y. Lin, and H. X. Jiang, *Appl. Phys. Lett.* **81**, 3365 (2002).

⁴ K. B. Nam, J. Li, M. L. Nakarmi, J. Y. Lin, and H. X. Jiang, *Appl. Phys. Lett.* **82**, 1694 (2003).

⁵ <http://www.phys.ksu.edu/area/GaNgroup>

⁶ K. B. Nam, J. Li, M. L. Nakarmi, J. Y. Lin, and H. X. Jiang, *Appl. Phys. Lett.* **81**, 1038 (2002).

⁷ M. Yoshikawa, M. Kunzer, J. Wagner, H. Obloh, P. Schlöter, R. Schmidt, N. Herres, and U. Kaufmann, *J. Appl. Phys.* **86**, 4400 (1999).

⁸ E. F. Schubert, I. D. Goepfert, W. Grieshaber, and J. M. Redwing, *Appl. Phys. Lett.* **71**, 921 (1997).

⁹ H. C. Casey and F. Stern, *J. Appl. Phys.* **47**, 631 (1976).

¹⁰ K. C. Zeng, J. Y. Lin, H. X. Jiang, and W. Yang, *Appl. Phys. Lett.* **74**, 3821 (1999).

¹¹ K. Pakua, M. Wojdak, M. Palczewska, B. Suchanek, and J. M. Baranowski, *MRS Internet J. Nitride Semicond. Res.* **3**, 34 (1998).